GOES EUVS Measurements

Janet Machol, NOAA National Centers for Environmental Information (NCEI) and University of Colorado, CIRES
Rodney Viereck, NOAA Space Weather Prediction Center (SWPC)
Andrew Jones, University of Colorado, LASP
12 August 2015, Version 3.1.1

Caution: The raw data **time stamps** are offset by 1-2 s after the integration periods. (See Section 3.1.1.) The 1-min average timestamps are *incorrectly* offset by about 11 s. (See Section 3.1.2.)

Version	Date	Change description	author
3.1.1	12 August 2015	Fixed error in Equation 2.	Machol
3.1	4 March 2015	original	Machol

Contents

1. Summary

The geostationary orbiting GOES 13-15 satellites were launched in 2006, 2009, and 2010 respectively. They each carry an Extreme Ultraviolet Sensor (EUVS) which measures the EUV in 5 bands (A-E) from about 5-127 nm as shown in Figure 1. The raw data is counts with a 10.24 s sample rate and a requirement of <15% uncertainty. The data comes from the NOAA Space Weather Prediction Center (SWPC) and is further processed and archived by the NOAA Geophysical Data Center (NGDC). NGDC currently provides calibrated data for the A, B and E bands for all three satellites. GOES 14 is unique in

that it measures duplicate A and B bands (with the A' and B' channels) instead of C and D bands, and this data is available as well. Times of available GOES EUVS measurements are shown in Figure 2.

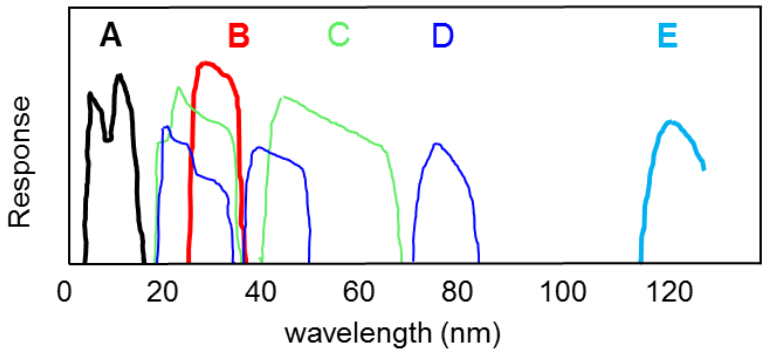

Figure 1. Wavelength responses of the GOES EUV sensors for the A-E bands.

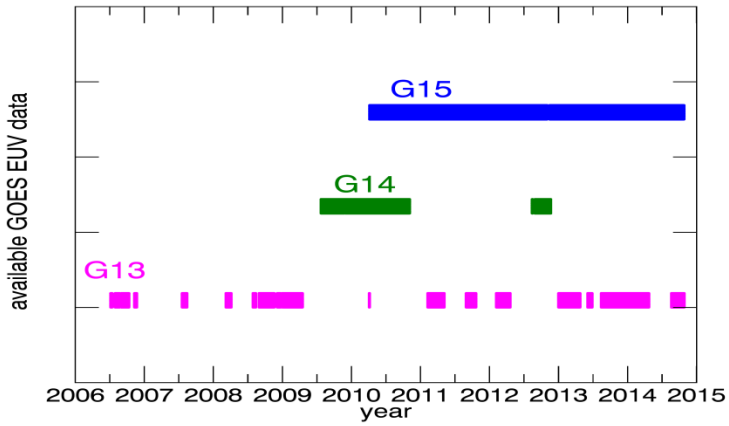

Figure 2. Available EUV measurements from GOES satellites.

The EUVS raw count data is converted into irradiances using measured detector response curves and quiet sun reference spectra. In general, measurements of the A and B bands agree well with other instruments and there has been no noticeable degradation. The E bands have noticeable degradation which varies between instruments and do not seem to have the correct conversion factor -- the Lyman-α values are too high. Therefore we scale the Channel E data by the SORCE SOLSTICE Lyman-α values with an exponential function that simultaneously corrects for degradation and the absolute value. The residual from this scaling is only a few percent, and so this process provides corrected 1 minute Lyman-α data from GOES based on daily Lyman-α from SOLSTICE. Figure 3 through Figure 5 show the measured irradiances for the A, B, and E bands.

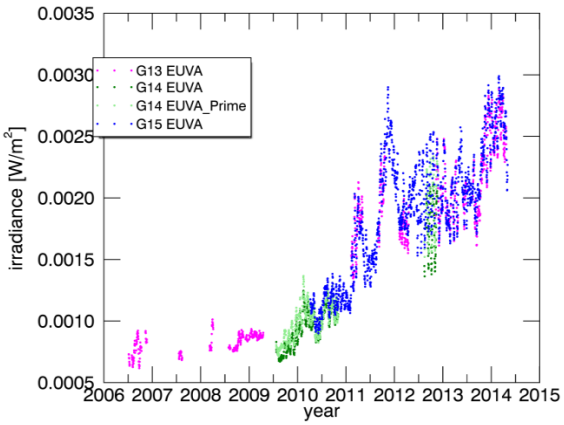

Figure 3. Irradiances for Channel A of GOES-13, -14 and -15. Irradiances for GOES-14 Channel A' are also shown.

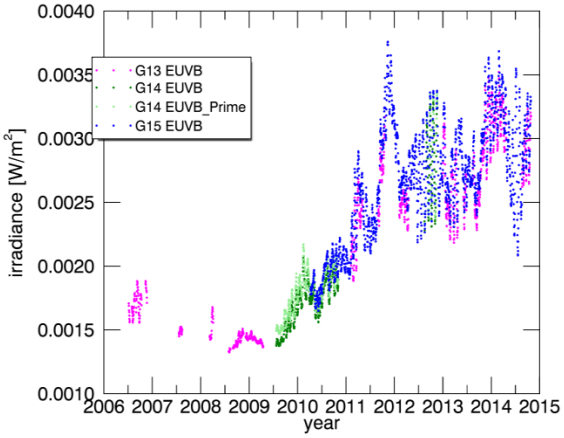

Figure 4. Irradiances for Channel B of GOES-13, -14 and -15. Irradiances for GOES-14 Channel B' are also shown.

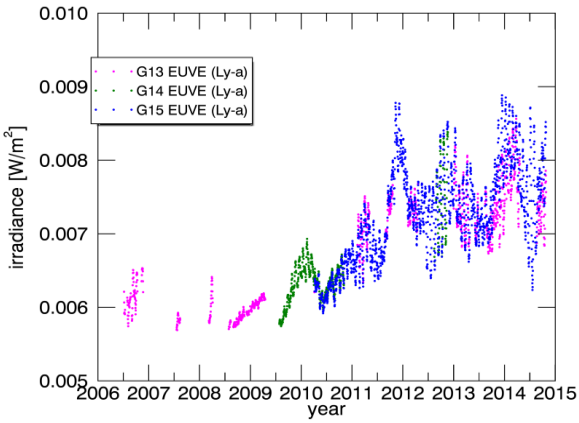

Figure 5. Daily irradiances from Channel E corrected to match the SORCE SOLSTICE Lyman-α band for GOES-13, -14 and -15.

2. Data access

The NGDC archive provides provides raw (10.24 s) counts and flags, calibrated ASCII data files with 1-min and daily averaged counts and irradiances. Column and format information is in the file headers. The E channel files also contain 1-min and daily irradiances which have been adjusted to a 1-nm bandpass around the Lyman-α line and which are scaled to SORCE SOLSTICE. The data archive also includes annual "quick look" plots. Most of the data is currently available up to October 2014. Data processing and file production is not yet automated, but the dataset will be updated periodically. Automation should occur by spring of 2016.

High cadence (10.24 s) irradiances can be created from the raw counts with the values with Equation 1 in conjunction with the tables in Appendix A. For Channel E, the degradation equation (Eq. 2) will need to be applied as well.

Count and irradiance data is not adjusted to 1 AU. However, the daily files contain 1 AU correction factors. Also, daily AU_correction files are provided separately and the factors in them can be interpolated for use with the 10-s and 1 min data.

The following archived files are available at the NGDC website. Table 1 lists the current data versions.

Yearly files of calibrated counts and irradiances for satellite (*nn*), channel (*c*), version (x), and year (*yyyy*)

http://satdat.ngdc.noaa.gov/sem/goes/data/new_avg/*yyyy*/new_euv_temp/goes*nn*/vx/

G*nn*_EUV*c*_*yyyy*_vx.txt	*1 minute data (counts, irradiances, and flags)*
G*nn*_EUV*c*_*yyyy*_daily_vx.txt	*daily data (counts, irradiances, and flags)*

Plots and multi-year data files are archived in the directory for the most recent year YYYY

http://satdat.ngdc.noaa.gov/sem/goes/data/new_avg/YYYY/new_euv_temp/

.../multi_year/G*nn*_EUV*c*_y_{start}_y_{end}_daily_vx.txt	*daily data combined for years y_{start} to y_{end}*
.../AU_corr/AU_correction_factor_daily.txt	*daily factors to convert data to 1AU, by doy*
.../AU_corr/AU_correction_factor_daily_2006_2020.txt	*daily factors to convert data to 1AU, by date*
.../plots_vx/ G*nn*_EUV*c*_irrad_yyyy_ vx.png	*1 year plot of 1 min and daily irradiances*

Raw data files with 10 s cadence counts

http://satdat.ngdc.noaa.gov/sem/goes/data/new_avg/*yyyy*/new_euv_temp/raw/

G*nn*_EUV*c*_Cnts_*yyyy*.dat	*raw 10s counts*
G*nn*_EUV*c*_Flags_*yyyy*.dat	*flags for raw 10s data*

Documentation

http://ngdc.noaa.gov/stp/satellite/goes/doc/

GOES_NOP_EUV_v2.pdf	GOES *EUVS readme file*
GOES_XRS_readme.pdf	*GOES XRS readme file*

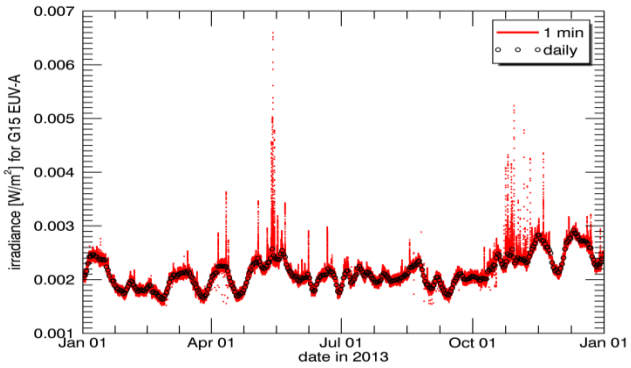

Figure 6. Irradiance plot with 1 min and daily averages for 2013 for GOES-15 Channel A. Plots like these are available in archive.

Figure 6 shows an example of a comparison of 1 min and daily irradiance value. Low points are due to imperfect removal of eclipse, offpoint, and calibration data. Eclipse seasons are April and October.

Table 1. Data versions. Latest versions in bold font.

sat ch	version	comments	latest data
15 A	**2**	corrected for heater noise	April 14
15 B	**2**		Oct 2014
15 E	2	scaled to SORCE SOLSTICE v12; use single exponential for fit use all 24 h for daily average and fit	Oct 2014
	3	excludes 8 h about LT midnight for daily average and fit; scaled to SORCE SOLSTICE v13; scaled with $y(t)=A_0 \exp[A_1(t- t0)] + A_2t + A_3$	Oct 2014
14 A	**2**	corrected for heater noise	2012
14 A'	**2**		2012
14 B	**2**		2012
14 B'	**2**		2012
14 E	2	scaled to SORCE SOLSTICE v12; use single exponential for fit; use all 24 h for daily average and fit; excludes data before Dec2009 in fit	2012
	3	excludes 8 h about LT midnight for daily average and fit; scaled to SORCE SOLSTICE v13; scaled with y(t)=A0 exp[A1(t- t0)] + A2t + A3; excludes data before Dec2009 in fit	2012
13 A	2	corrected for heater noise	April 2014
13 B	2		Oct 2014
13 E	2	correction inadequate - data should not be used for now scaled to SORCE SOLSTICE v12; use single exponential for fit use all 24 h for daily average and fit	Oct 2014
	3	correction inadequate - data should not be used for now excludes 8 h about LT midnight for daily average and fit; scaled to SORCE SOLSTICE v13; scaled with y(t)=A0 exp[A1(t- t0)] + A2t + A3	Oct 2014

3. Data calibration and processing

3.1 Calibration

Count data is converted to calibrated fluxes with the equation:

$$\text{EUV Channel Irradiance } [W/m^2] = ((\text{Counts} - B\ [\text{counts}]) * G\ [\text{A/count}] - V\ [\text{A}]) / C\ [\text{A}/(W/m^2)] \quad \text{(Eq. 1)}$$

where for each channel, *B* is the background, *G* is the gain, *V* is the visible light contamination, and *C* is a units conversion factor. The values for the *G* and *V* come from the GOES Data and Calibration Handbooks. The background values, *B*, are really electronic offsets, and are determined from the measurements when the satellite is pointed away from the Sun. The conversion factors are determined from a convolution of the measured detector spectral responses with a quiet sun spectrum and change with solar activity level (Appendix B2). Calibration factors are given in the tables of Appendix A.

3.1.1 Raw data

The EUVS channels accumulate counts for 10.24 s. As shown in Figure 7, for Channels A and B, the time stamps are 1.024 s after the end of the accumulation, while for Channels C-E, the time stamps are 2.048 s after the end of the accumulation. Integration periods for different channels are not concurrent.

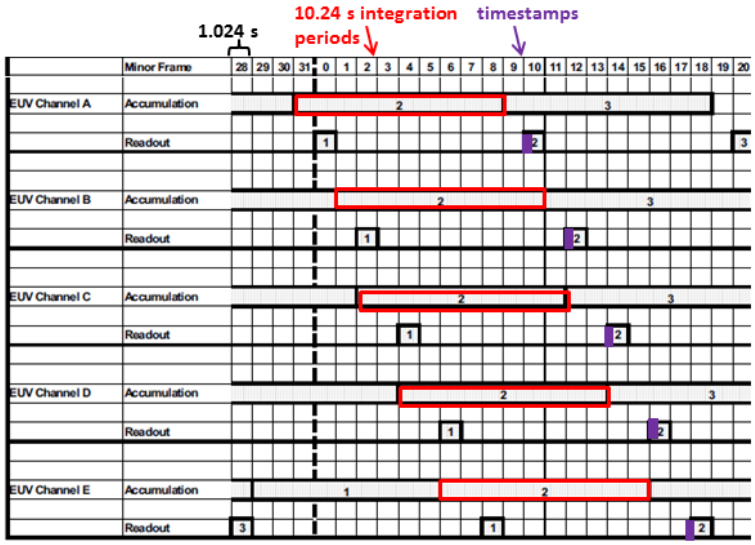

Figure 7. Sketch of EUVS instrument timing. Telemetry minor frames are 1.024 s. Integration is 10.24 s and timestamps occur 1.024 or 2.048 s after the end of the integration, depending on channel.

SWPC has provided flags for bad/missing data, off-pointing, calibrations and eclipses for the raw data since 2010. These flags are shown in Table 2.

Table 2. Flags for 10-s count data. Real count values are denoted as *x*.

flag	definition	counts
0	no flag	*x*
-99999	bad or missing data	-99999
1048576	in-flight calibration	*x*
2097152	off-pointed	*x*
3145728	off-pointed and in-flight calibrations	*x*
4194304	Sun is eclipsed by the Moon	*x*
8388608	Sun is eclipsed by the Earth	*x*
12582912	Sun is eclipsed by the Moon and the Earth	*x*
14680064	Sun has unknown eclipsed (Moon or Earth)	*x*

3.1.2 Averages of 1 minute

The 1-min averaged data is created from averages of the raw count data excluding spikes, dropouts, and data with bad flags are excluded. The A channel counts are also cleaned of noise from the Solar X-ray Imager (SXI) heater as described in Appendix B2. The averaged irradiances are created from the averaged counts with Eq. 1.

The 10-s flags are combined to create flags for the minute data files in Table 3. The 'partial eclipse flag' is set for data near eclipse periods to indicate that the counts are reduced by thermal effects. The number of minutes of partial eclipse flags set on either side of an eclipse depends empirically on the eclipse duration. Partial eclipse flags are set for 8 mins before and 5 mins after eclipse periods longer than 30 mins, and for 12 mins before and 10 mins after eclipse periods shorter than 30 mins.

Each 10-s record with good data is averaged into the 1 min period in which its midpoint lies. Timestamps for 1-min data are in middle of the period. **However, for the present data version, the 10-s timestamp offsets were incorrectly assumed to be at the start of the accumulations instead of 1-2 s beyond the ends. Therefore the averaged data has timestamps which are late by about 11 s.** These timestamps will be corrected in the next data version. The raw data spacing is 10.24 s, and so 97% of the 1-min averages contain 5 or 6 raw records. About 3% of the 1-min records have no data (flags 5, 8 or -999).

Table 3. Flags and values in 1-min averaged data. Actual counts or irradiance values are denoted as *x*.

flag	definition	flags in 10-s source records	counts	irradiance
0	no flag	all data in average had flag=0 and no partial eclipse	*x*	*x*
1	possible bad data	Used in GOES14 Chan E before 1 December 2010 when there is a different degradation rate based on fit to SOLSTICE Lyman-α data; included in daily values	*x*	*x*
2	partial eclipse	Flag set to 0 in 1-minute average routine. Later analysis adds partial eclipse flags near times with eclipses.	*x*	*x*
5	eclipse	At least one eclipse flag (flag >4,000,000) and no off-point or calibration flags.	-999	-999.0
8	off-pointed or in-flight calibrations	At least one off-point or calibration flag (1,000,000 < flag < 4,000,000)	-999	-999.0
-999	bad or missing data	all flags were -99999	-999	-999.0

3.1.3 Daily averages

The daily data contains averages of 1 min data and has flags of either 0 or 1. There are only three flags options for the daily averages as shown in Table 4. Timestamps are the middle of the integrated period.

For the channel E data, the daily average excludes times within ±4 h of local midnight, in order to exclude absorption dips near midnight due to geocoronal hydrogen absorption. The impacts are biggest at the equinoxes. The dips range from about 0.3 to 6% and are largest around the equinoxes. Excluding the dips results in about a 1% change in the daily averages.

Table 4. Flags and values in daily averaged data. Actual counts or irradiance values are denoted as *x*.

flag	definition	flags in 10-s source records	counts	irradiance
0	no flag	all data in average had a 1 min flag of 0	*x*	*x*
1	possible bad data	all data in average had 1 min flags of 0 or 1	*x*	*x*
-999	bad or missing data	no average because there were no 1 min flags of 0 or 1	-999	-999.0

3.2 Channel E degradation and Lyman-α

Channel E data is converted to a 1 nm band around the Lyman-α line at 121.6 nm by scaling based on the LASP WHI quiet sun reference spectrum. The scaling factor is about 88% (Table 7 in Appendix A). The E channel suffers degradation, and so to remove the degradation, the data is scaled to SORCE SOLSTICE Lyman-α measurements. The ratio of the daily averaged GOES Lyman-α to the daily SOLSTICE Lyman-α is fit for version 3 data with the function:

$$y(t) = A_0 \exp[A_1 \cdot (t - t_0)] + A_2 \cdot (t - t_0) + A_3 \qquad \text{(Eq. 2)}$$

The daily and one minute GOES Lyman-α data is then divided by this function which scales the data to SOLSTICE and corrects for degradation. The amount of degradation for Channel E as a function of year is given in Table 5. The factors for the scaling function are given in Table 12 and Table 13 in Appendix A.

Table 5. Amount of degradation for Channel E after a given number of years from launch date based on the fit parameters in Table 13.

	after: 1 year	2 years	5 years
GOES13	1%	3%	7%
GOES14	14%	16%	16%
GOES15	11%	18%	32%

4. Future improvements to the data

There are number of refinements that should be done on the EUVS data processing. These include:

- Automate file creation.
- Correct time stamps in 1 minute averaged data.
- Consider using other reference spectra.
- Determine how best to apply reference spectra that vary with solar activity.
- Create flags for years prior to 2010.
- Determine best way to combine duplicate A and B channels on GOES 14 to get cleaner data.
- Process Channels C and D on GOES 13 and 15.
- Improve correction for GOES-13 Channel E data.
- Create composites with data from all three satellites.

References

Viereck, R., F. Hanser, J. Wise, S. Guha, A. Jones, D. McMullin, S. Plunket, D. Strickland, S. Evans (2007), "Solar extreme ultraviolet irradiance observations from GOES: design characteristics and initial performance", Proc. SPIE 6689, Solar Physics and Space Weather Instrumentation II, 66890K, doi:10.1117/12.734886.

Warren, H.P.(2005), Astrophys. J. Suppl. Ser. 157, 147. doi:10.1086/427171.

Data Sources

LASP WHI spectra http://lasp.colorado.edu/lisird/whi_ref_spectra/
NRL Spectrum

Contacts

Please contact janet.machol@noaa.gov for comments and questions regarding the archived GOES EUVS data or this document, or if you wish to be added to a mailing list for updates on the GOES EUVS data set.

Appendix A. Calibration Tables

The tables in Appendices A1, A2, and A3 are used with Eq. 1 to convert count rates into irradiances. The scale factors in the tables can be used to scale the bandpasses of the GOES channels to match the bandpasses of other instruments. Table 12 provides the fit parameters to correct for degradation in the Channel E Lyman-α data for all three satellites.

A1. Tables for GOES 13

Table 6. Correction factors for GOES 13. Gain and background values are for a telescope temperature of 12C. Background is used as an offset.

channel	Background [counts]	Gain [A/counts]	Visible Light Contamination [A]	bandpass [nm]
A	25198	1.91E-15	2.13E-14	2.8-20.6
B	15970	1.89E-15	1.21E-14	2.8-36.4
C	16229	1.90E-15	4.79E-14	-
D	24387	1.89E-15	1.20E-15	-
E	25096	1.90E-15	1.32E-12	113.5-132.8

Table 7. Flux conversion factors, *C*, for GOES-13 channels for solar minimum and maximum conditions. Also shown are scale factors, *f*, to match the bandpasses of other instruments.

channel	solar activity	C[A/(W/m^2)]	f_{EVE} 5-15 nm	f_{EVE} 25-34 nm	f_{SOHO} 26-34 nm	$f_{Lyman-\alpha}$ 121.0-121.9 nm
A	minimum	8.918e-10	0.21	-	-	-
A	maximum	8.065e-10	0.19	-	-	-
B	minimum	6.615e-09	-	0.406	0.368	-
B	maximum	6.034e-09	-	0.381	0.335	-
E	minimum	2.612E-09	-	-	-	0.884

A2. Tables for GOES 14

Table 8. Correction factors for GOES 14. Gain and background values are for a telescope temperature of 12C. Background is used as an offset.

channel	Background [counts]	Gain [A/counts]	Visible Light Contamination [A]	bandpass [nm]
A	26571	1.92E-15	1.04E-14	2.8-19.0
B(A')	23948	1.93E-15	7.18E-14	2.8-19.0
C (B)	14207	1.93E-15	2.96E-13	6.0-36.6
D (B')	24856	1.95E-15	5.47E-14	6.0-36.6
E	25188	1.94E-15	2.49E-12	113.7-135.9

Table 9. Flux conversion factors, *C*, for GOES-14 channels for solar minimum and maximum conditions. Also shown are scale factors, *f*, to match the bandpasses of other instruments.

channel	solar activity	C[A/(W/m^2)]	f_{EVE} 5-15 nm	f_{EVE} 25-34 nm	f_{SOHO} 26-34 nm	$f_{Lyman-\alpha}$ 121.0-121.9 nm
A	minimum	8.718e-10	0.256	-	-	-
A	maximum	8.691e-10	0.248	-	-	-
A'	minimum	8.744e-10	0.256	-	-	-
A'	maximum	8.628e-10	0.248	-	-	-
B	minimum	4.841e-09	-	0.424	0.385	-
B	maximum	4.441e-09	-	0.406	0.357	-
E	minimum	2.630e-09	-	-	-	0.855

A3. Tables for GOES 15

Table 10. Correction factors for GOES 15. Gain and background values are for a telescope temperature of 12C. Background is used as an offset.

channel	Background [counts]	Gain [A/counts]	Visible Light Contamination [A]	bandpass [nm]
A	49454	1.91E-15	1.78E-14	3.6-20.8
B	49797	1.90E-15	2.71E-14	3.6-38.5
C	55451	1.90E-15	2.03E-15	-
D	51218	1.90E-15	4.37E-14	-
E	40947	1.90E-15	2.23E-12	116.3-132.4

Table 11. Flux conversion factors, *C*, for GOES-15 channels for solar minimum and maximum conditions. Also shown are scale factors, *f*, to match the bandpasses of other instruments.

channel	solar activity	C[A/(W/m^2)]	f_{EVE} 5-15 nm	f_{EVE} 25-34 nm	f_{SOHO} 26-34 nm	$f_{Lyman-\alpha}$ 121.0-121.9 nm
A	minimum	1.100e-09	0.213	-	-	-
A	maximum	1.006e-09	0.193	-	-	-
B	minimum	3.786e-09	-	0.399	0.363	-
B	maximum	3.594e-09	-	0.379	0.333	-
E	minimum	2.348e-09	-	-	-	0.884

A4. Lyman-α fit parameters

Table 12. Version 2 fit parameters for the to the function $y(t)=A_0 \exp[A_1(t- t_0)] + A_2$ for time, *t*, in units of Julian Day. The Lyman-α data from Channel E is corrected for degradation and scaled to SOLSTICE by dividing by this function. The fit for GOES14 starts on 1 Dec 2009. Values in blue are changed in version 3 from previous version 2. *We do not recommend using the GOES13 Channel E data until we determine more corrections to it.

	A_0	A_1	A_2	t_0 [Julian Day]
GOES13*	0.22656203	-0.00032264091	0.92886897	2454302
GOES14	0.071629217	-0.0064360812	1.0913027	2455037
GOES15	0.42309890	-0.00098659526	0.88899175	2455168

Table 13. Version 3 fit parameters for the to the function $y(t)=A_0 \exp[A_1(t- t_0)] + A_2 t + A_2$ for time, *t*, in units of Julian Day. The Lyman-α data from Channel E is corrected for degradation and scaled to SOLSTICE by dividing by this function. The fit for GOES14 starts on 1 Dec 2009. Values in blue are changed in version 3 from previous version 2. *We do not recommend using the GOES13 Channel E data until we determine more corrections to it.

	A_0	A_1	A_2	A_3	t_0 [Julian Day]
GOES13*	-0.017348879	-0.00048805848	-5.0711674e-005	1.1609864	2453857
GOES14	0.20591992	-0.0059919019	-5.6673415e-007	1.0750063	2454984
GOES15	0.12569144	-0.0034349324	-0.00016150714	1.1978867	2455257

Appendix B. Processing Procedure

B1. Channel A temperature correction

The GOES NOP EUV-A Channel data has noise spikes that are correlated with the Imager Mounting Platform (IMP) heater. The heater keeps the IMP at a stable temperature and has fixed set points that are not controllable from the ground. During the coldest parts of the GOES season (summer), the heaters cycle about every 10 – 50 minutes. During the warmest parts of the GOES season (winter) the heaters are sometimes not required at all and may stay off for weeks at a time.

A temperature gradient across two dissimilar metal components of the IMP may be producing very small currents that get into the EUV-A detector signal current. Thus, as the IMP is warmed by the heater, a reverse current combined with the detector current makes the EUV-A net signal go down. When the heater goes off, the plates cool, and the current goes the other way, thus increasing the signal from the detector. Only the EUV optical housing that is mounted closest to the IMP seems to experience this heater noise, and within that housing, only the A channel is noticeably affected. In some of the EUVS sensors, the heater noise can also be seen in the B channel (mounted in the same housing) but this noise is vastly reduced and is therefore not removed from the signal.

The heater noise is partially removed from the GOES EUV-A data by using the SXI PCM2 temperature sensor as a proxy for the heater with a routine developed by R. Viereck. The SXI PCM2 temperatures are sampled about every 30 s. To process these data, the noise spikes and outliers are removed from the count data and then a 7 point or 3.5 minute box-car smoothing is applied. The first derivative of the temperature is then calculated. This first derivative looks similar to the heater noise in the EUV-A signal and is scaled to fit the EUV-A signal. A small time shift of the SXI PCM2 data is required to maximize the fit of the SXI PCM2 data to the EUV-A data but this shift and the scaling remain constant throughout the mission. An example of the Channel A data with the heater noise and the heater noise correction is shown in Figure 8.

The smoothing and the time-shifting of the SXI PCM2 data make it impossible to calculate the correction in real-time; however, the delay introduced by this process is less than 5 minutes. For GOES-15, the impact of the heater noise has not changed since launch. Heater noise corrections were done for GOES 13 and 15 only, because on GOES-14, there is SXI heater data only for 2009. On GOES 14, the A channel is expected to be much more impacted than the A' channel.

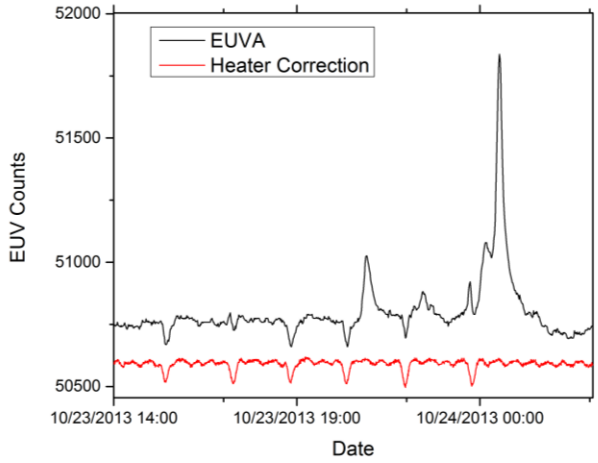

Figure 8. Channel A counts (black) showing heater noise and correction (red) based on SXI heater current.

B2. Calibrations

The original calibrations in the Handbook were done by ATC with the EUV beam at Brookhaven National Laboratory. The background values, *B*, do not vary much in time after the initial few months. We rederived these values by looking at measurements when the instrument was pointing away from the sun. We also rederived the conversion values, *C*, since the ones in the Handbook are of poor quality; they were created with a flat spectrum and are given in the wrong units --- [A/(W/m^2-nm] instead of [A/(W/m^2]. Previously, SWPC applied additional empirical correction factors in the conversion from counts to fluxes; these are no longer used.

Currently we do calibrations with quiet sun spectra. For the shorter wavelengths (channels A-D) we use the NRLEUV 2 updated Model Quiet Sun Irradiance Spectrum (Warren, 2005), while for the Channel E around Lyman-α we use the LASP WHI quiet sun spectrum. Response curves for the channels A, B and E for GOES-15 are shown in Figure 9 through Figure 13 along with reference spectra for a quiet sun during solar minimum and maximum. The responses for the different satellites are similar but not identical.

More details such as impacts of solar activity, angle, particle backgrounds and limb effects could be considered. In the future, comparisons should be done for regimes based on solar activity, at least a quiet regime and a flare regime. Assuming solar maximum instead of solar minimum conditions can result in a 10% increase in the irradiance. However, when the bandpasses are scaled to match other instruments, sometimes the variability in f sometimes almost exactly cancels the variability in C, and so the net ratio between the instrument measurements does not change significantly.

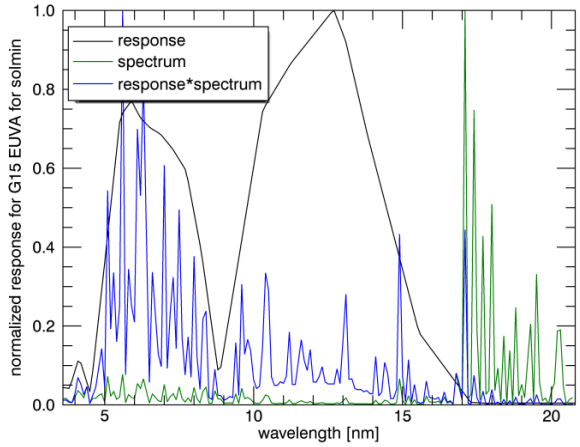

Figure 9. Response curve, solar minimum spectrum and response*spectrum for Channel A on GOES 15.

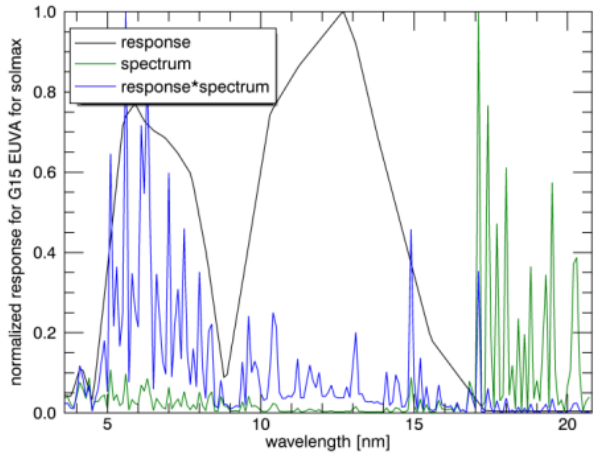

Figure 10. Same but for solar maximum for Channel A.

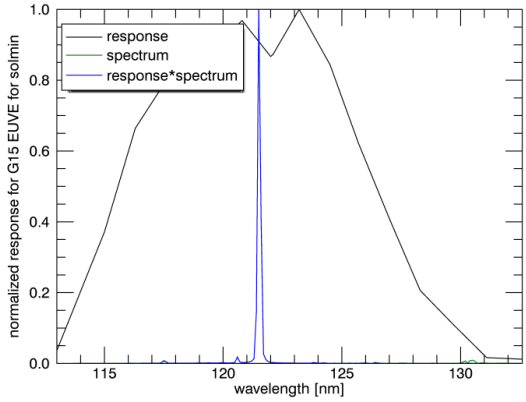

Figure 13. Same but for solar minimum for Channel E.

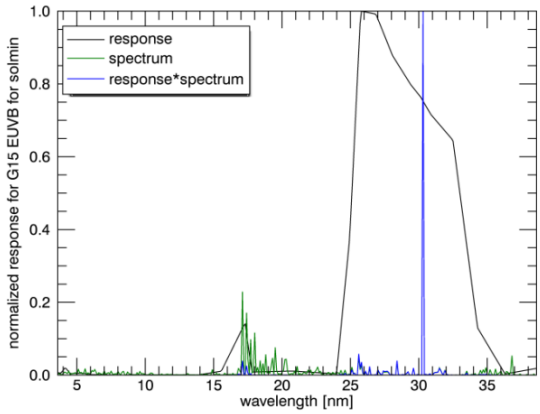

Figure 11. Same but for solar minimum for Channel B.

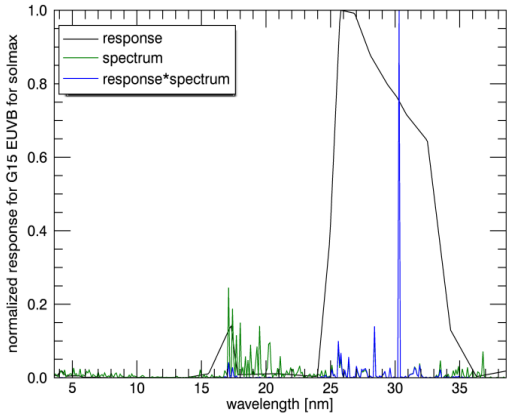

Figure 12. Same but for solar maximum for Channel B.

After applying a 1 AU correction to the data, it is compared with daily values from other instruments to test the calibrations. SDO EVE data was used for Channel A comparisons, SDO EVE and SOHO SEM data were used for Channel B, and SORCE SOLSTICE Lyman-α was used for Channel E comparisons. The equations for the calibrations are given below.

The photon irradiance values are given per 0.5 nm. Let's convert these to W m^{-2}. The resolution of 0.5 nm does not impact the equations; it is carried through.

The photon irradiance J_i are in units of [γ cm^{-2} s^{-1} $(0.5\ nm)^{-1}$]
The desired units are J_i[W m^{-2} $(0.5\ nm)^{-1}$].

E/photon= hc/λ[m] γ^{-1}= $hc/(\lambda$[nm] · 10^{-9}[m/nm]) γ^{-1}
with h=6.626x10^{-27} erg ·s, c = 3 x 10^8 m s^{-1}, and 1 W= 10^7 erg s^{-1}

The conversion is then

J_i[W m^{-2} $(0.5\ nm)^{-1}$] = J_i [γ cm^{-2} s^{-1} $(0.5\ nm)^{-1}$] · $hc/(\lambda$[nm] · 10^{-9}[m/nm]) γ^{-1}

$$= \frac{J_i\ [\gamma\ cm^{-2}\ s^{-1}\ (0.5\ nm)^{-1}]\ \gamma^{-1} \cdot 10^9\ [nm\ m^{-1}] \cdot (6.626 \times 10^{-27}\ erg \cdot s \cdot 3 \times 10^8\ m\ s^{-1})\ (1W \cdot 10^{-7}\ erg^{-1}\ s) \cdot [10^4\ cm^2 \cdot m^{-2}]}{\lambda[nm]}$$

$$= \frac{J_i\ [cm^{-2}\ s^{-1}\ (0.5\ nm)^{-1}] \cdot\ 1.988 \times 10^{-12}\ [(cm^2\ s\ nm)\ (W\ m^{-2})]}{\lambda[nm]}$$

For the quiet regime, the total irradiance over the band is given by

$$J_{tot\_quiet}\ [W\ m^{-2}] = \sum_i J_i[\mathrm{W\ m^{-2}\ (0.5\ nm)^{-1}}]$$

The current for the quiet time is given by

$$I_{tot\_quiet}[A] = \sum_i\ R_i[A\ m^2\ W^{-1}]\ \cdot\ J_i[\mathrm{W}\ m^2\ (0.5\ \mathrm{nm})^{-1}]$$

So now, if we measure a current, I_{meas}, during a quiet time, then the total flux in the band is

$$J_{tot\_meas} = (J_{tot\_quiet} / I_{tot\_quiet}) \cdot I_{meas}$$

To compare with another instrument on a different type of satellite, we scale the total flux by the fraction of the flux that is in the bandpass of the other instrument. We can also estimate the fraction of irradiance in energy units in some band subset with

$$f_{subset} = \sum_i J_i[\mathrm{W\ m^{-2}\ (0.5\ nm)^{-1}}]\ /\ J_{tot\_quiet}\ [W\ m^{-2}]$$ where i is in subset

Appendix C. Comparisons with other satellite data

This section shows time series of GOES irradiances as well as comparisons with the following calibrated data sets: SDO EVE, version 4; SOHO SEM, version 3; and SORCE SOLSTICE Lyman-α, version 12. To compare the irradiance for the GOES Channels A and B with irradiance from another satellite instrument we estimated the fraction of the GOES channel irradiance that would fall in the other instrument bandpass as described in Appendix B4. The GOES data was adjusted to 1 AU for the comparisons with the other data sets. The SOHO SEM data has 17-nm scatter into this band which sometimes results in a double-humped peak for each solar rotation since it is has an angular factor (A. Jones, personal communication). Major sources of discrepancies between data sets are calibration errors, incomplete correction for differing bandpasses, and the use in the GOES calibrations of solar minimum reference factors instead of factors that vary with solar activity.

C.1 GOES-15

C.1.1 GOES 15 Channel A

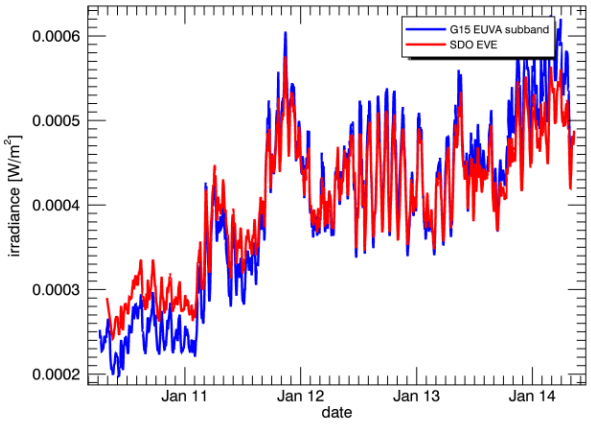

Figure 14. Comparison of the EVE GOES-A band (derived from MEGS A for the 5 to 15 nm band) with a subset of the GOES-15 Channel A data from 5-15 nm.

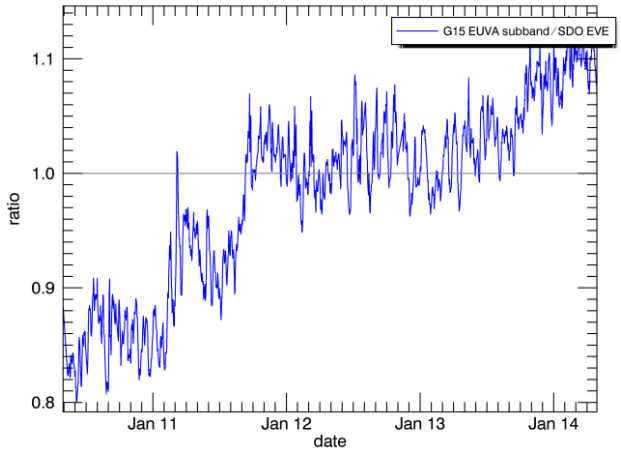

Figure 15. Ratio of GOES-15 EUV-A to EVE GOES-A band.

4.1.2 GOES-15 Channel B

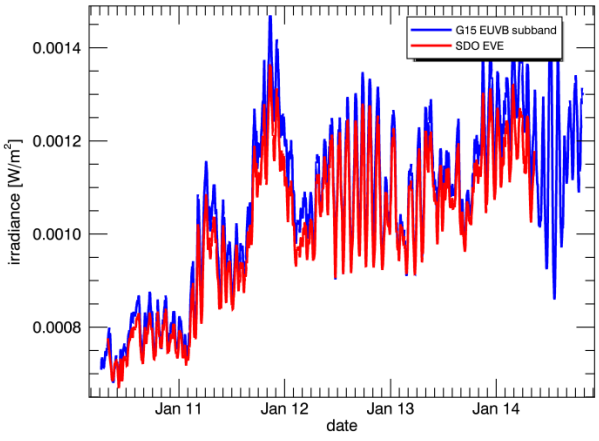

Figure 16. Comparison of the EVE GOES-B band with subset of the GOES-15 Channel B data from 25-34 nm.

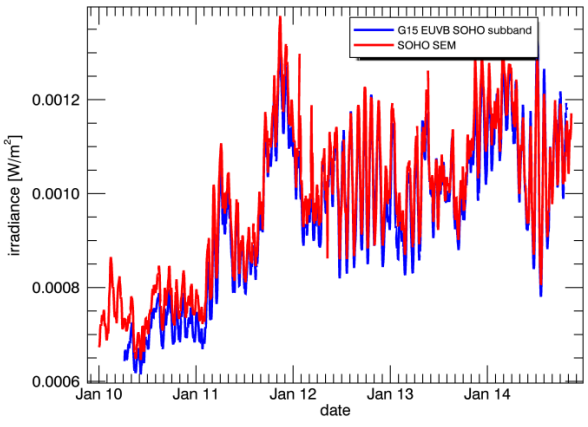

Figure 17. Comparison of the SOHO SEM 26-34 nm band with subset of the GOES-15 Channel B data from 26-34 nm.

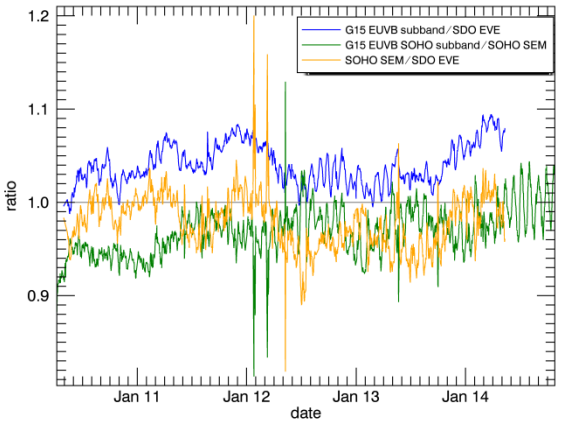

Figure 18. Ratios between GOES 15 EUVS-B, SDO EVE, and SOHO SEM.

C.1.3 GOES-15 Channel E

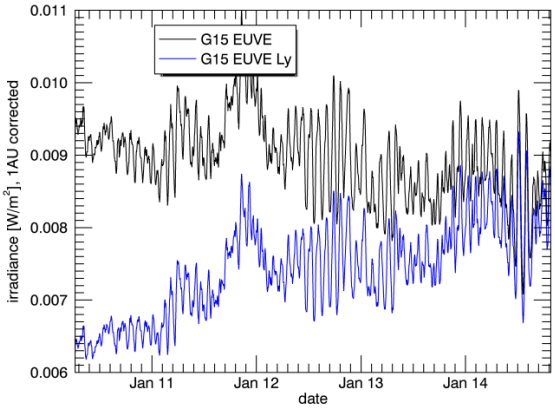

Figure 19. The GOES-15 EUVS-E data and the 1 nm Lyman-α subband (121.0 -121.9 nm) before degradation correction.

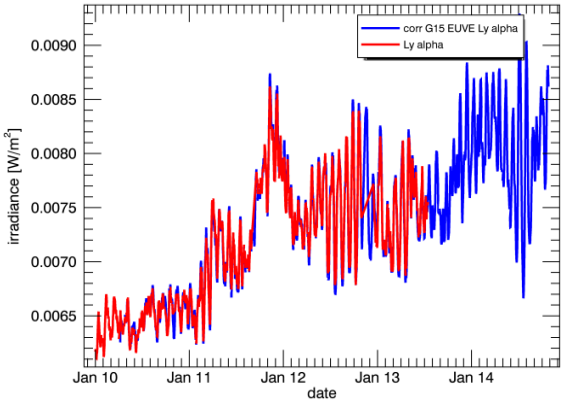

Figure 20. Comparison of the scaled and degradation-corrected GOES-15 Channel E data from 121.0-121.0 nm to the SORCE SOLSTICE Lyman-α.

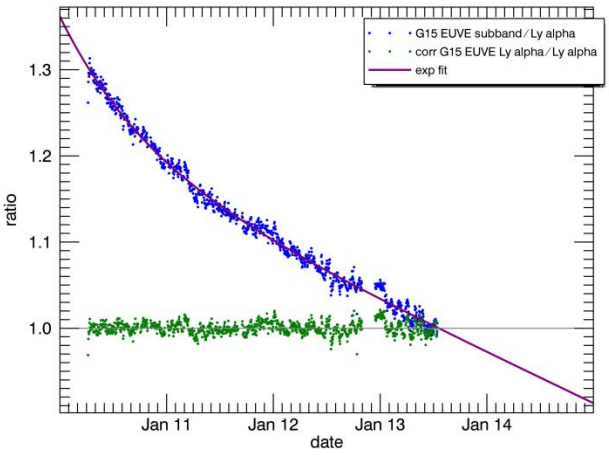

Figure 21. Ratio of GOES-15 EUVS-E to the SOLSTICE elements of the SORCE SOLSTICE Lyman-α (blue dots). The ratio is fit (purple line) with the function $y=a \bullet \exp[b(t-t_0)] + c$. This fit is used both to determine the decay rate and to correct the data. The anomalous period from 1 Dec 2012 to 20 Jan 2013 was excluded for the fit generation. The residual (green dots) is <±3%.

C.2 GOES-14

C.2.1 GOES-14 Channels A and A'

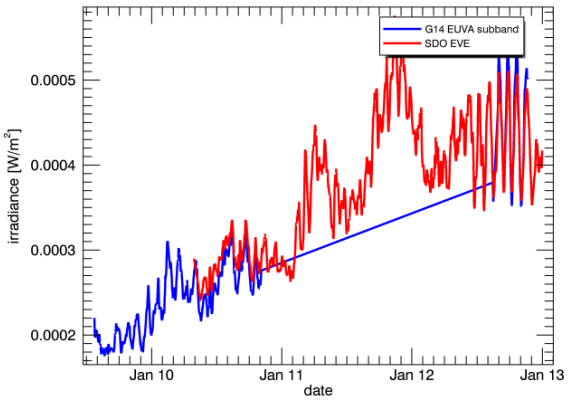

Figure 22. Comparison of the EVE GOES-A band (derived from MEGS A for the 5 to 15 nm band) with a subset of the GOES-14 Channel A data from 5-15 nm.

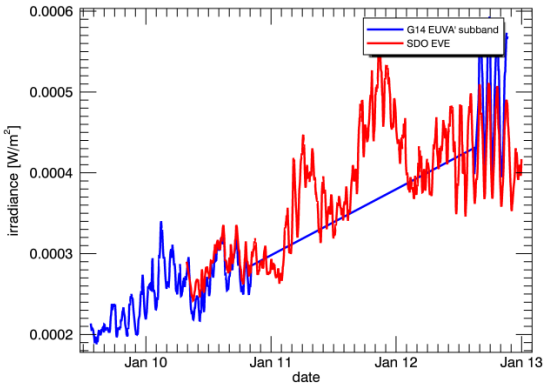

Figure 23. Comparison of the EVE GOES-A band (derived from MEGS A for the 5 to 15 nm band) with a subset of the GOES-14 Channel A' data from 5-15 nm.

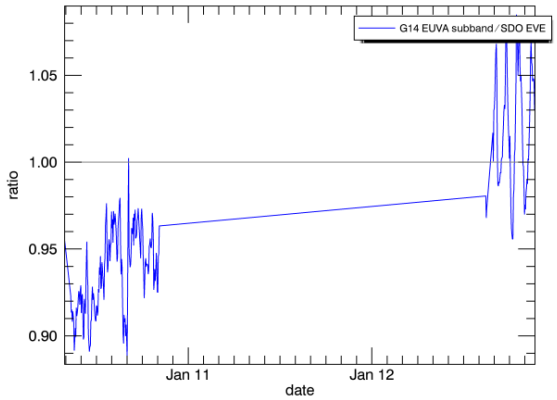

Figure 24. Ratio of GOES-15 EUV-A to EVE GOES-A band.

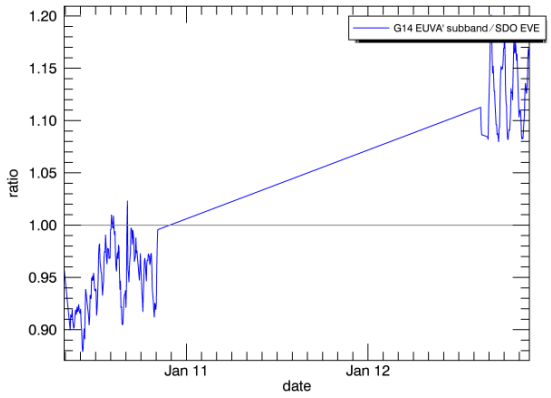

Figure 25. Ratio of GOES-15 EUV-A' to EVE GOES-A band.

C.2.2 GOES-14 Channels B and B'

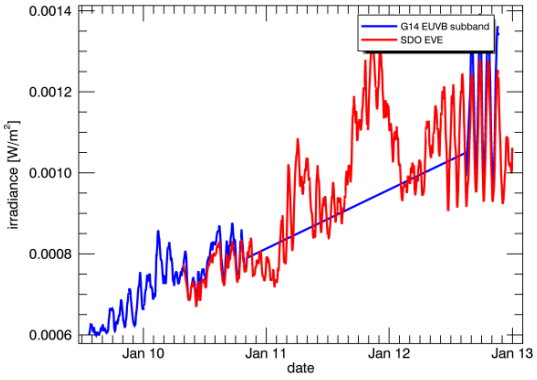

Figure 26. Comparison of the EVE GOES-B band with subset of the GOES-14 Channel B data from 25-34 nm.

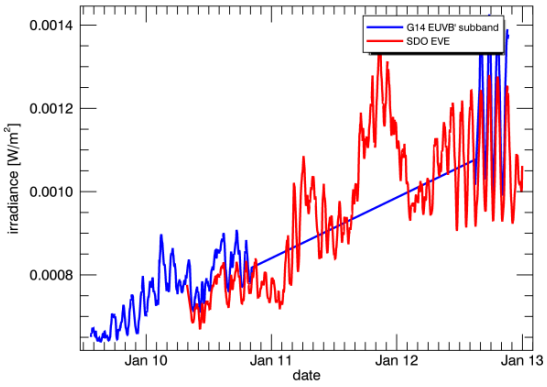

Figure 27. Comparison of the EVE GOES-B band with subset of the GOES-14 Channel B' data from 25-34 nm.

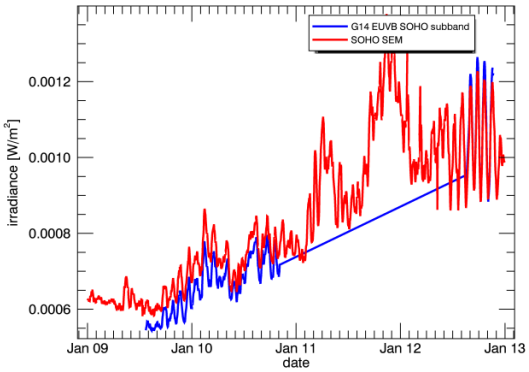

Figure 28. Comparison of the SOHO SEM 26-34 nm band with subset of the GOES-14 Channel B data from 26-34 nm.

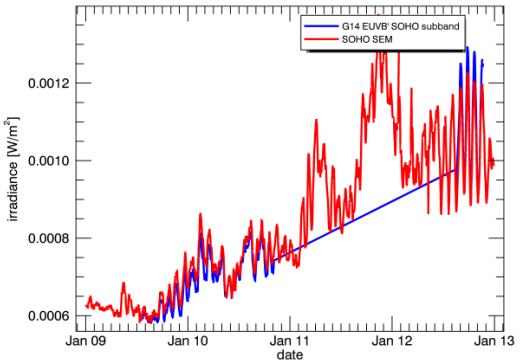

Figure 29. Comparison of the SOHO SEM 26-34 nm band with subset of the GOES-14 Channel B' data from 26-34 nm.

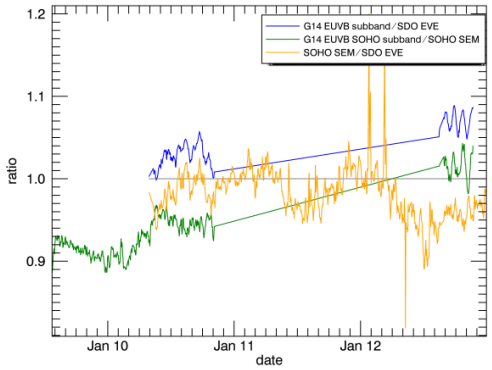

Figure 30. Ratios between GOES 14 EUVS-B, SDO EVE, and SOHO SEM.

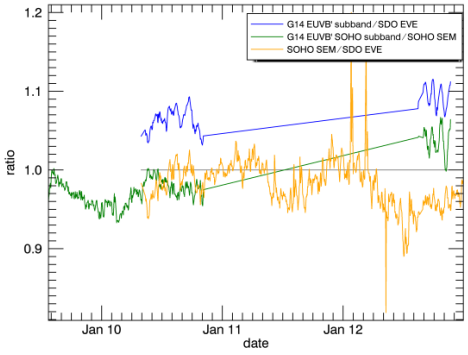

Figure 31. Ratios between GOES 14 EUVS-B', SDO EVE, and SOHO SEM.

C.2.3 GOES-14 Channel E

The Channel E measurements prior to 1 Dec 2009 has a much slow decay and the reason for this is not known, and so the degradation fit is started on that date. Flags are set to 1 for the early time period to note that it has a questionable calibration.

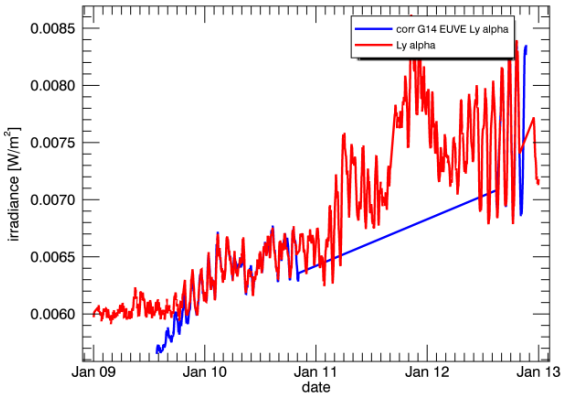

Figure 32. Comparison of the scaled and degradation-corrected GOES-14 Channel E data from 121.0-121.0 nm to the SORCE SOLSTICE Lyman-α.

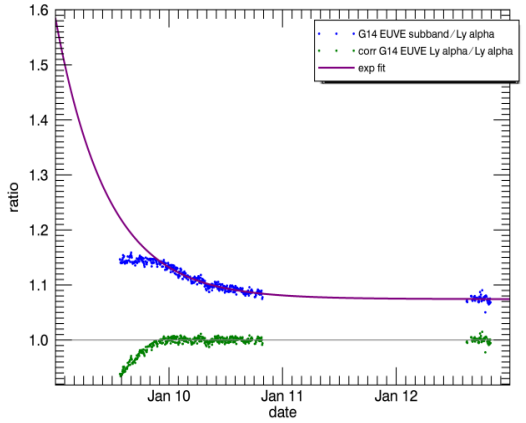

Figure 33. Ratio of GOES-14 EUVS-E to the SOLSTICE elements of the SORCE SOLSTICE Lyman-α (blue). The fit (purple) and residual (green) are shown.

C.3 GOES-13

C.3.1 GOES-13 Channel A

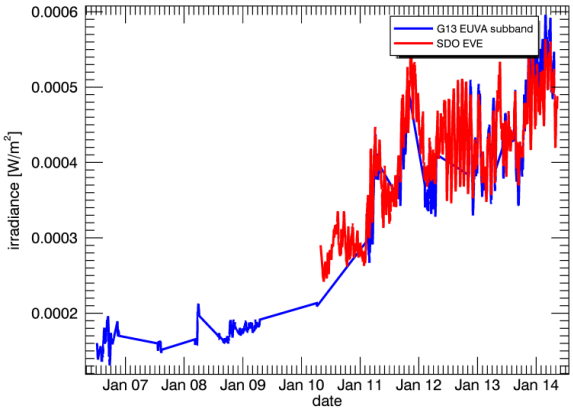

Figure 34. Comparison of the EVE GOES-A band (derived from MEGS A for the 5 to 15 nm band) with a subset of the GOES-13 Channel A data from 5-15 nm.

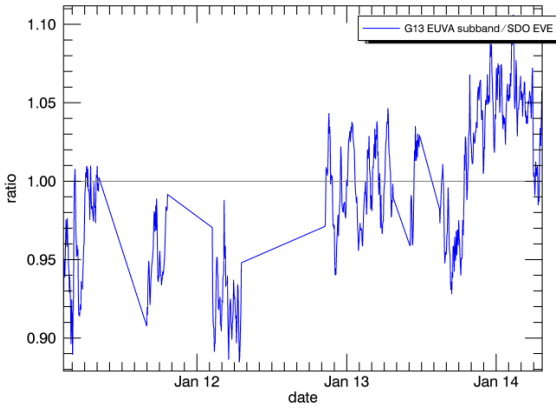

Figure 35. Ratio of GOES-13 EUV-A to EVE GOES-A band.

C.3.2 GOES-13 Channel B

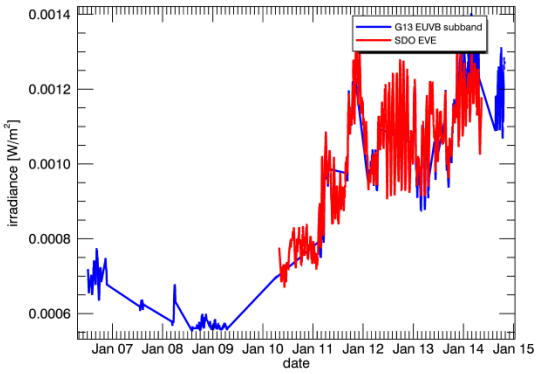

Figure 36. Comparison of the EVE GOES-B band with subset of the GOES-13 Channel B data from 25-34 nm.

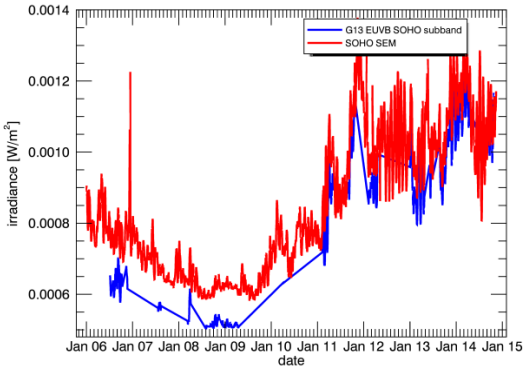

Figure 37. Comparison of the SOHO SEM 26-34 nm band with subset of the GOES-13 Channel B data from 26-34 nm.

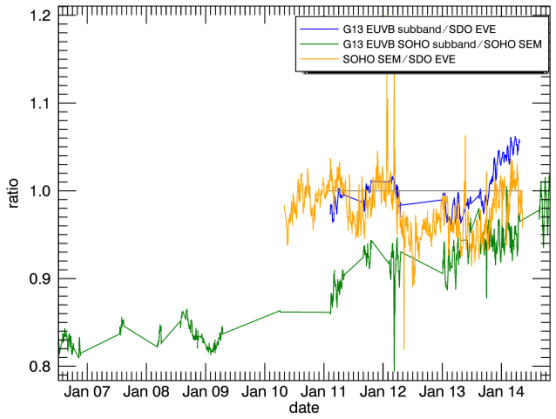

Figure 38. Ratios between GOES 13 EUVS-B, SDO EVE, and SOHO SEM.

C.3.3 GOES-13 Channel E

More work needs to be done to correct the GOES-13 Channel E data and this data should not be used.

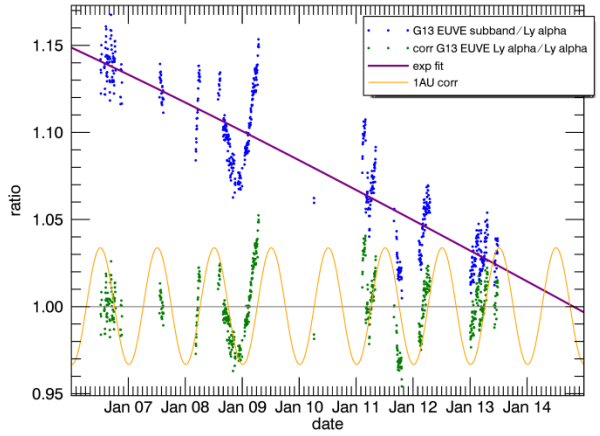

Figure 39. Ratio of GOES-13 EUVS-E to the SOLSTICE elements of the LASP Lyman-α Composite (blue dots). The ratio is fit (purple line) with the function y=a•exp[b(t-t0)] + c. The 1AU correction is shown as a guide to the eye for possible future seasonal temperature corrections.

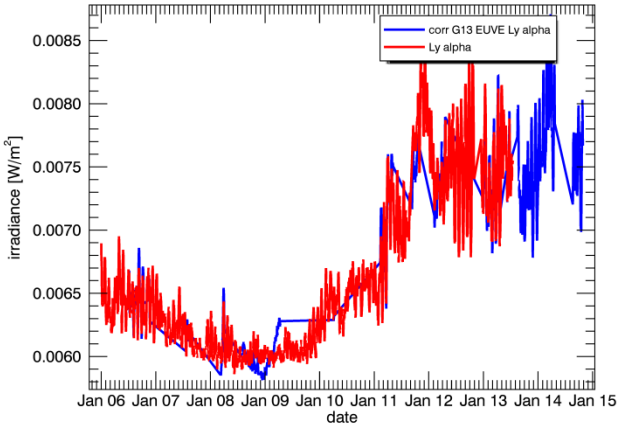

Figure 40. Comparison of the scaled and degradation-corrected GOES-13 Channel E data from 121.0-121.0 nm to the SORCE SOLSTICE Lyman-α.

Appendix D. GOES EUVS hardware

The EUVS on GOES-13-15 were all very similar. The five channels of the EUV were measured via three spectrograph units with east-west dispersion. The units vary in the grating spacing, For GOES 13 and 15, the first unit measure channels A and B and the second unit measures channel s C and D. For GOES 14, the first unit measures channels A and B, and the second unit measures channels A' and B'. The measurements are redundant except that the A'-B' detectors are arranged in opposite order so that they have opposite impacts of angular effects from sources near the solar limb. The intent is that each pair of channels can be averaged to produce an irradiance with reduced error due to angular effects. For all three GOES satellites, Channel E is measured on a separate spectrograph. Sample rates are once every 32.768 s. Table 14 shows some details of the spectrograph elements, specifically the hardware design, manufacturer, components, contamination and degradation.

Table 14. Hardware components for EUVS on GOES 13-15. Note that on GOES-14, the C and D channels are at the usual A and B wavelengths.

instrument/component	manufacturer	details
EUVS	ATC	There are 3 optical benches: one for A and B, one for C and D (or A' and B' on GOES-14), and one for E. Nominal wavelengths (nm) are: A: 5-15, B: 25-34, C: 17-67, D: 17-84, E: 118-127
detectors	IRD	AXUV photodiode On GOES-14,channels B, B' and E are nitrided.
gratings	MIT	A,B: 5000 lines/mm C,D: 2500 lines/mm E: 1667 lines/mm
thin film filters on detectors	Lebow	A: 50/200/70 nm of Ti/Mo/C B: 150/5 nm of Al/Al_2O_3 C: 150/2 nm of Al/Al_2O_3 D: 150/2 nm of Al/Al_2O_3
Lyman-α filter	Acton Labs	free standing

Several design features and manufacturing techniques were incorporated to minimize the impact of contamination (Viereck et al., 2007). The first optical component is the transmission grating. The buildup of contaminants from outside the sensor will occur primarily on the grating bars which will have minimal impact on the transmission properties. The grating can accumulate 10's of nm of molecular contaminants before experiencing a noticeable change in transmission whereas an optical component such as a filter or window will exhibit a significant decrease in performance (depending on the material) for more than about 0.5 nm of contaminants. To minimize the contaminants on internal optical surfaces, the EUVS was manufactured in a clean environment. The few electronic components and wires required to control and read the silicon diodes are at the back of the optical housing and are kept extremely clean. The entire package was stored with a dry nitrogen purge or in a vacuum during most of its testing and prelaunch storage activities. Zeolite absorbers inside the optical housing are designed to capture any residual contaminants that remain inside the optical housing after launch.